

## Robust Retrieval of Dynamic Sequences through Interaction Modulation

Lukas Herron

*Biophysics Program and Institute for Physical Science and Technology, University of Maryland, College Park, Maryland 20742, USA*

Pablo Sartori \*

*Instituto Gulbenkian de Ciência, 2780-156 Oeiras, Portugal*

BingKan Xue †

*Department of Physics and Institute for Fundamental Theory, University of Florida, Gainesville, Florida 32611, USA*



(Received 3 April 2023; accepted 27 November 2023; published 22 December 2023)

Many biological systems dynamically rearrange their components through a sequence of configurations in order to perform their functions. Such dynamic processes have been studied using network models that sequentially retrieve a set of stored patterns. Previous models of sequential retrieval belong to a general class in which the components of the system are controlled by feedback (input modulation). In contrast, we introduce a new class of models in which the feedback modifies the interactions among the components (interaction modulation). We show that interaction modulation models not only are capable of retrieving dynamic sequences, but they do so more robustly than input modulation models. In particular, we find that modulation of symmetric interactions allows retrieval of patterns with different activity levels and has a much larger dynamic capacity. Our results suggest that interaction modulation may be a common principle underlying biological systems that show complex collective dynamics.

DOI: [10.1103/PRXLife.1.023012](https://doi.org/10.1103/PRXLife.1.023012)

### I. INTRODUCTION

Biological systems are often made of many components that dynamically arrange themselves into specific configurations. In some cases, this dynamics follows a particular sequence of configurations which allows the system to perform some function, as illustrated in Fig. 1. For example, neurons rearrange their neural activity in order to generate a sequence of activity patterns [1,2]. Multiprotein assemblies dynamically rearrange their protein composition several times in a precise order as they perform a function, such as the spliceosome processing pre-mRNAs [3]. Bacterial communities on marine particles undergo successions where the species structure changes in reproducible patterns to degrade organic matter [4]. Thus, sequential transitions of multicomponent systems through well-defined configurations is a general phenomenon in biology.

These specific configurations can be considered metastable states of the dynamics. The ability of the system to transition from one such configuration to the next means that the system can alter the stability of the configurations. This can be achieved by controlling specific components, e.g., by

changing the abundance of certain proteins in the case of assembly dynamics, or by modulating the neuron firing activity in neural systems. Such a scenario corresponds to a common approach in control theory, i.e., modulating inputs on a subset of variables to influence the full system [5]. In biology, however, a different approach may be considered, namely, to modify the interactions among the components. Unlike physical systems where the interactions between elementary particles are determined by fundamental forces, biological components are complex objects and the effective interaction strengths between them can be modified by third parties. For example, the affinity between a pair of proteins can be regulated by allosteric modulation through a third protein [6]. Similarly, the synapses among a pair of neurons can be modulated by a third neuron via heterosynaptic plasticity [7]. Can such interaction modulation be used to control the dynamics of complex systems? What are the differences in performance between interaction and input modulation?

In this work we address these questions using a framework inspired by the Hopfield neural network [8]. The Hopfield network was originally developed as an abstract model of associative memory capable of storing and retrieving particular network configurations. This paradigm has been extended to model biological systems ranging from metabolic networks [9] to protein assemblies [10] and even ecosystems [11]. Furthermore, sequential transitions among the stored configurations have long been considered [12–15], aimed at describing phenomena such as central pattern generation [16], counting [17], and, more recently, free association [18], memory recall [19], and assembly dynamics [20]. Here we model the dynamics of retrieval by introducing a small set of

\*Corresponding author: psartori@igc.gulbenkian.pt

†Corresponding author: b.xue@ufl.edu

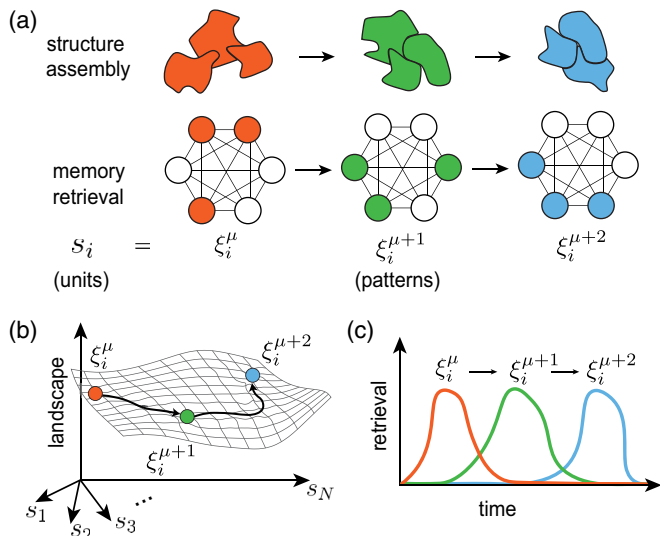


FIG. 1. Sequential dynamics in complex systems. (a) Sequential transition along a sequence of configurations is a common phenomenon in complex systems, such as the assembly of multiprotein complexes and the synaptic activity of neurons. Such dynamics may be modeled by a network where the units  $s_i$  store multiple patterns  $\xi^\mu$ . (b) Sequential dynamics can be viewed as unfolding across a rugged, changing landscape. (c) Transitions between configurations are represented by time series of order parameters, which measure how close the system is to each configuration. The peak of each colored curve represents the retrieval of a particular configuration.

feedback units, which control the sequential transitions. When formulated this way, previous models are shown to fall into a class of models based on input modulation. We propose a new class of models that rely on interaction modulation to trigger autonomous transitions between configurations. Remarkably, we find that modulation of symmetric interactions allows sequential retrieval of configurations that have different activity levels, which cannot be reliably done by models that use input modulation. Furthermore, this model can retrieve much longer sequences than other models. Our results suggest that interaction modulation may be biologically favored over input modulation due to its robustness and large dynamic capacity.

## II. BACKGROUND

Our model is based on the classic Hopfield network, which can store and retrieve a given set of network configurations, or patterns. The network is composed of  $N$  units, whose activities are denoted by  $\{s_i\}_{i=1}^N$  and take continuous values  $0 \leq s_i \leq 1$ . The interactions among the units are characterized by a matrix  $W_{ij}$ , which contributes to the input of each unit:

$$h_i = \sum_{j=1}^N W_{ij} s_j + V_i. \quad (1)$$

Here  $V_i$  is an external input to each unit that does not depend on the current state  $s_i$  of the network. The dynamics of the system is governed by

$$\dot{s}_i = -s_i + F(h_i), \quad (2)$$

where  $F(\cdot)$  is an activation function, which we choose to be the Heaviside step function for simplicity.

The original task of a Hopfield network is to store and retrieve  $p$  patterns, denoted by  $\{\xi^\mu\}_{\mu=1}^p$ , each of which is a vector with binary elements,  $\xi_i^\mu \in \{0, 1\}$ . The patterns can represent structured content, such as the pixels of black-and-white images, but for simplicity we take them to be random with an average activity  $a$ . Specifically, each pattern has a fraction  $a$  of the units set to 1 and the rest set to 0. To store those patterns, the following symmetric interactions are introduced [8]:

$$J_{ij} = \frac{1}{Na(1-a)} \sum_{\mu=1}^p (\xi_i^\mu - a)(\xi_j^\mu - a). \quad (3)$$

For  $W_{ij} = J_{ij}$  and  $V_i = 0$ , the patterns will be fixed points of the dynamics in Eq. (2) (as long as the total number of patterns is far below the storage capacity). In other words, the system will retrieve a pattern provided it is close to it initially, where the proximity to patterns is measured by the  $p$  overlap variables,

$$m^\mu = \frac{1}{Na(1-a)} \sum_i (\xi_i^\mu - a)s_i. \quad (4)$$

Thus, for  $s_i = \xi_i^1$ , we have  $m^1 = 1$  and  $m^{\mu \neq 1} \approx 0$ , because random patterns are approximately orthogonal for large  $N$ . Equations (1)–(3) define a dynamical system capable of storing and retrieving each individual pattern.

We are interested in networks that can autonomously retrieve a sequence of patterns, one after another. Already in Hopfield's original paper [8], it was suggested that sequential retrieval could be achieved by introducing asymmetric interactions of the form

$$\tilde{J}_{ij} = \frac{1}{Na(1-a)} \sum_{\mu} (\xi_i^{\mu+1} - a)(\xi_j^\mu - a). \quad (5)$$

These asymmetric interactions provide a directional bias from every pattern  $\xi^\mu$  towards the next pattern  $\xi^{\mu+1}$ . The interaction matrix is then generalized to  $W_{ij} = J_{ij} + \lambda \tilde{J}_{ij}$ , where the parameter  $\lambda$  represents the strength of the directional bias. The rationale behind this construction is that, after a pattern is retrieved due to the symmetric  $J_{ij}$  term, the asymmetric  $\tilde{J}_{ij}$  term will destabilize it and push the system toward the next pattern in the sequence, i.e.,  $\xi^1 \rightarrow \xi^2 \rightarrow \xi^3 \dots$ .

However, this simple model cannot produce sequences reliably [8]. Instead, the network exhibits no dynamics for  $\lambda$  less than a certain value, or chaotic dynamics otherwise [21]. The reason is that the  $J_{ij}$  and  $\tilde{J}_{ij}$  terms act on the same timescale such that either the stabilizing term dominates and leads to no dynamics or the destabilizing term dominates and leads to chaotic dynamics. Therefore, robust sequential dynamics requires a separation of timescales between fast stabilization and slow destabilization. This will allow the system to first relax to a pattern  $\xi^\mu$ , which is slowly destabilized, then go to the next pattern  $\xi^{\mu+1}$ , and so on, as we demonstrate below.

## III. RESULTS

The required separation of timescales can be achieved through feedback modulation. To this end, we introduce a set

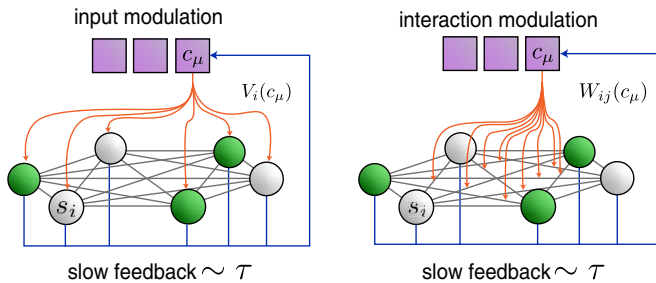


FIG. 2. Input versus interaction modulation. A Hopfield network with units  $s_i$  (spherical nodes) is controlled by a set of feedback units  $c_\mu$  (square nodes). These feedback units are updated on a slow timescale  $\tau$  (blue lines) and modulate either the input field  $V_i$  of the main units or their interactions  $W_{ij}$  (orange lines).

of feedback units represented by the variables  $\{c_\mu\}_{\mu=1}^p$ , which obey the dynamics

$$\dot{c}_\mu = -\frac{1}{\tau}(c_\mu - m^\mu). \quad (6)$$

This form of dynamics can be equivalently expressed as a weighted average of the past network state, i.e.,  $c_\mu = \int_{-\infty}^t K(t-t') \sum_i W_{\mu i} s_i(t') dt'$  with  $K(t) \propto e^{-t/\tau}$  and  $W_{\mu i} \propto \xi_i^\mu - a$ . Our results are insensitive to the exact form of the kernel  $K$  as long as it has a slow timescale  $\tau \gg 1$ , such as a step function (resulting in an average over a period  $\tau$ ) or a delta function (resulting in a time delay  $\tau$ ) [12]. The specific projection matrix  $W$  that we use can be considered as arising from a learning process that associates each feedback unit with a particular pattern, similar to the slow learning dynamics modeled in Ref. [22].

These feedback units  $c_\mu$  will be used to destabilize the retrieved pattern by modifying the inputs to either the network, i.e.,  $V_i(c_\mu)$ , or the interactions,  $W_{ij}(c_\mu)$ , as schematically depicted in Fig. 2. We will elaborate on these two approaches below, with four representative models summarized in Table I (see also Fig. 3).

### A. Sequential retrieval via input modulation

We first reformulate some well-studied models of sequential retrieval using our framework. For instance, the model due to Horn and Usher [13] can be reexpressed by setting  $W_{ij} = J_{ij} + \lambda \tilde{J}_{ij}$  and  $V_i = -\theta \sum_\mu \xi_i^\mu c_\mu$ . The latter is usually referred to as an adaptive threshold, with  $\theta$  the strength of inhibition. In this model neurons that are active in a retrieved pattern will experience an inhibitory input after a time approximately equal to  $\tau$ , which tends to turn them off and thus

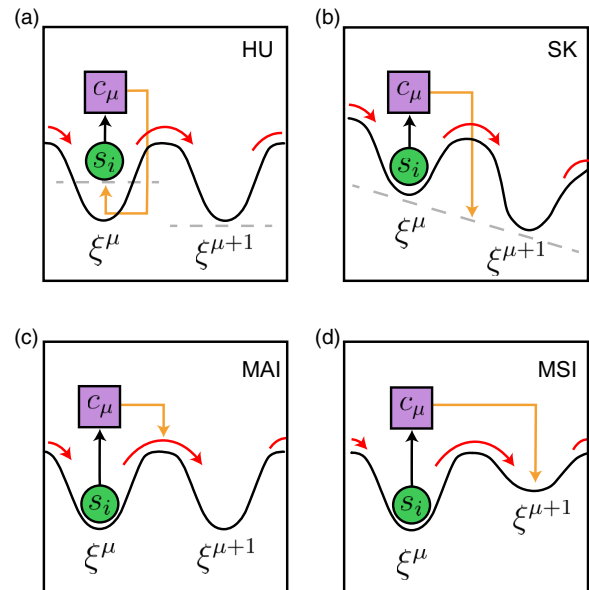


FIG. 3. Heuristic depictions of the models considered in Table I in terms of a slowly changing energy landscape. The network state  $s_i$  currently occupies the pattern  $\xi^\mu$  and will transition to  $\xi^{\mu+1}$ . The local minima represent the patterns stored through symmetric interactions, the red arrows represent asymmetric interactions that bias the transitions, and the dashed lines represent thresholds (not shown when constant). The black arrows represent update to the feedback units  $c_\mu$  on a slow timescale and the orange lines represent the effect of the feedback. The input modulation models work by (a) raising the inhibitory threshold (HU) or (b) tilting the energy landscape (SK), whereas the interaction modulation models work by (c) enforcing the directional bias (MAI) or (d) deforming the energy landscape (MSI).

destabilize the current pattern. This model uses separate terms to serve different purposes: The symmetric interactions  $J_{ij}$  stabilize each pattern, the external field  $V_i$  slowly destabilizes the retrieved pattern through the feedback coupling, and the asymmetric interactions  $\tilde{J}_{ij}$  bias the system towards the subsequent pattern. Figure 4(a) shows an example of sequential retrieval using this model (more examples are shown in the Supplemental Material [23], Fig. S1).

Similarly, we can reformulate the model due to Sompolinsky and Kanter [12] through identifying  $W_{ij} = J_{ij}$  and  $V_i = \lambda \sum_\mu (\xi_i^{\mu+1} - a) c_\mu - \theta$ . In this model, after the network retrieves a pattern, the feedback units  $c_\mu$  slowly activate to drive the system towards the subsequent pattern. This is enough to destabilize the current pattern if  $\lambda$  is sufficiently large (see Sec. III C for feasible parameter regions). An example

TABLE I. Examples of input modulation (HU and SK) and interaction modulation (MSI and MAI) studied in this work.

Model	Interaction $W_{ij}$	Input $V_i$	Feedback through $c_\mu$
HU	$J_{ij} + \lambda \tilde{J}_{ij}$	$-\theta U_i(c_\mu)$	$U_i(c_\mu) \equiv \sum_\mu \xi_i^\mu c_\mu$
SK	$J_{ij}$	$\lambda U_i(c_\mu) - \theta$	$U_i(c_\mu) \equiv \sum_\mu (\xi_i^{\mu+1} - a) c_\mu$
MAI	$J_{ij} + \lambda \tilde{J}_{ij}(c_\mu)$	$-\theta$	$\tilde{J}_{ij}(c_\mu) \equiv \frac{1}{Na(1-a)} \sum_\mu (\xi_i^{\mu+1} - a)(\xi_j^\mu - a) c_\mu$
MSI	$J_{ij}(c_\mu) + \lambda \tilde{J}_{ij}$	$-\theta$	$J_{ij}(c_\mu) \equiv \frac{1}{Na(1-a)} \sum_\mu (\xi_i^{\mu+1} - a)(\xi_j^{\mu+1} - a) c_\mu$

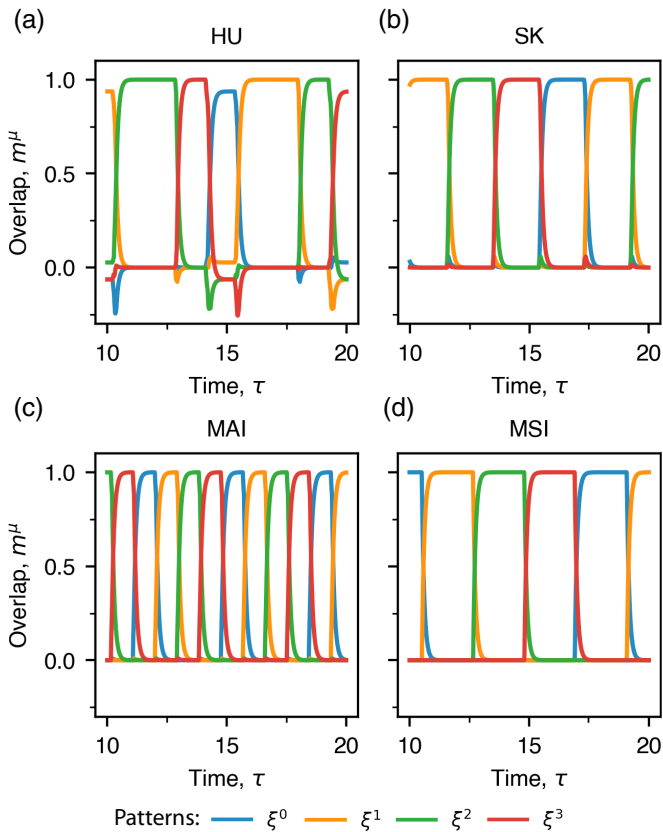


FIG. 4. Examples of dynamic retrieval for input and interaction modulation models: the (a) HU and (b) SK models that belong to the input modulation class and modulation of (c) asymmetric interactions (MAI) and (d) symmetric interactions (MSI). Each model stores a cyclic sequence of four orthogonal patterns ( $p = 4$ ). Each color represents the overlap with a particular pattern  $\xi^\mu$ , which is retrieved when the overlap  $m^\mu$  approaches 1. As different overlaps sequentially increase and decrease, the patterns are retrieved one after another, corresponding to retrieval of the stored sequence ( $\xi^0 \rightarrow \xi^1 \rightarrow \xi^2 \rightarrow \dots$ ). The parameters used for each model correspond to the green dots in Fig. 5 (SK,  $\lambda = 1.2$  and  $\theta = 0.37$ ; HU,  $\lambda = 0.3$  and  $\theta = 0.62$ ; MAI,  $\lambda = 1.7$  and  $\theta = 0.325$ ; and MSI,  $\lambda = 0.1$  and  $\theta = 0.06$ ).

of this dynamics is shown in Fig. 4(b) (more examples in Fig. S1 [23]).

### B. Sequential retrieval via interaction modulation

Our reformulation of both models above makes it clear that in these models the feedback units  $c_\mu$  modulate the input  $V_i$  to achieve sequential retrieval. We now present new models of sequential retrieval in which the feedback units  $c_\mu$  modulate the interactions  $W_{ij}$ . Two types of such modulation are possible, which act either on the symmetric interactions  $J_{ij}$  or on the asymmetric interactions  $\tilde{J}_{ij}$ .

First consider a model for the modulation of the symmetric interactions (MSI), which can be described by

$$J_{ij}(c_\mu) = \frac{1}{Na(1-a)} \sum_{\mu} (\xi_i^{\mu+1} - a)(\xi_j^{\mu+1} - a)c_\mu. \quad (7)$$

When the network has retrieved a pattern  $\xi^v$  for a period of time, all  $c_\mu$  will decay to zero except  $c_v$ . As a consequence,

all terms in  $J_{ij}$  will be turned off except for  $\mu = v$ . Therefore, only one pattern  $\xi^{v+1}$  will be stable, which is the one that the network will retrieve subsequently. In other words, the symmetric interactions store and retrieve one pattern at a time. Asymmetric interactions  $\tilde{J}_{ij}$  are needed to provide directional bias towards subsequent patterns, even though the strength  $\lambda$  can be small (see Sec. III C).

Alternatively, feedback units can be used to modulate the asymmetric interactions (MAI). Consider a model with

$$\tilde{J}_{ij}(c_\mu) = \frac{1}{Na(1-a)} \sum_{\mu} (\xi_i^{\mu+1} - a)(\xi_j^{\mu} - a)c_\mu. \quad (8)$$

As before, when the network has retrieved a pattern  $\xi^v$  for some time,  $c_v$  reaches a large value while all other  $c_\mu$  decay to zero. In this model, however, only one directional bias is active, corresponding to the transition  $\xi^v \rightarrow \xi^{v+1}$ . For a sufficiently large  $\lambda$ , this term will destabilize the current pattern and push the system towards  $\xi^{v+1}$ . Compared to the MSI model above, here all patterns are stored in the symmetric interactions, but only one transition is enabled at a time.

In Figs. 4(c) and 4(d) we show two examples of sequential retrieval using the MSI and MAI models, respectively (more examples in the Supplemental Material [23], Fig. S2). As one can see, the dynamic trajectories are very similar to the Horn-Usher (HU) and Sompolinsky-Kanter (SK) models, which operate via input modulation. We therefore conclude that interaction modulation is an equally feasible way of retrieving dynamic sequences.

### C. Phase space of sequential dynamics

Within our general framework, all models of sequential retrieval are characterized by the same two parameters: the magnitude of the bias  $\lambda$  and the threshold  $\theta$ . This allows us to compare interaction and input modulation by systematically examining the  $(\lambda, \theta)$  parameter space and identifying the regions in which sequential retrieval occurs. To proceed, we numerically solve the dynamical system and used a custom-made score for the dynamics to quantify the accuracy of sequential retrieval (see Appendix A for details).

Figure 5 presents  $(\lambda, \theta)$  plots for different levels of activity  $a$  in each of the four models. Shaded regions correspond to parameter combinations that produce sequential dynamics and regions within the red contour correspond to high accuracy (above 0.9). It can be seen that both input and interaction modulation models have compact regions of parameter space that allow sequential dynamics. However, the HU model is the least robust compared to others, as small parameter changes lead to dysfunctional behavior, such as dynamics with very high frequencies or pattern-dependent amplitudes and frequencies (see Fig. S1 [23]).

To better visualize the dependence of model performance on the activity level  $a$ , we overlaid the regions of accurate retrieval (red contours in Fig. 5) from different  $a$  values, as shown in the last column of Fig. 5. The HU model has very small retrieval regions for any  $a$ . For SK and MAI the retrieval region drifts from a positive value of  $\theta$  towards 0 as  $a$  increases. Notably, for MSI there is a compact region where the retrieval regions for different values of  $a$  overlap.

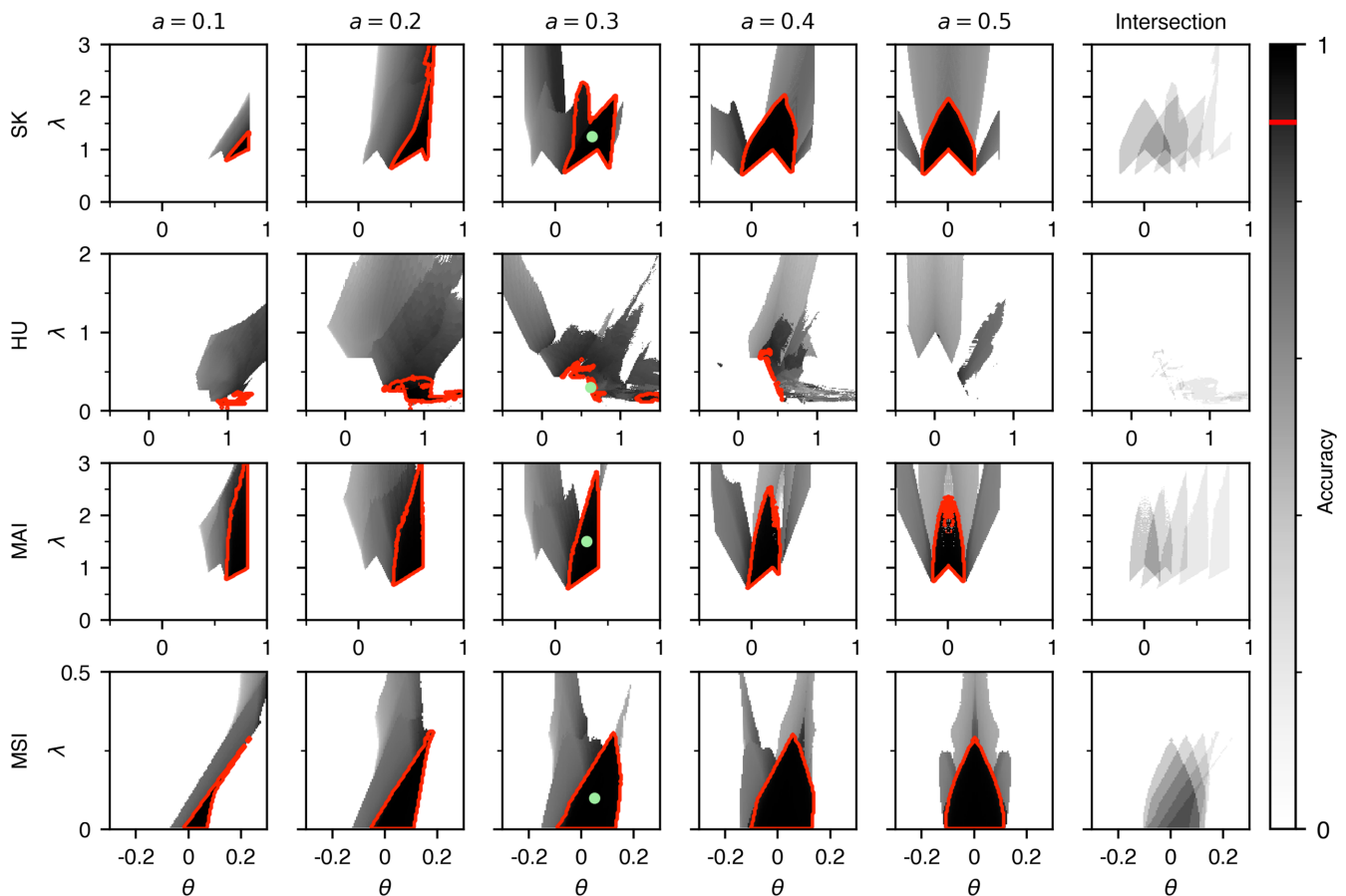


FIG. 5. Parameter space of sequential retrieval. The performance of each model for retrieving a cyclic sequence of four orthogonal patterns is evaluated at different combinations of the bias  $\lambda$  and threshold  $\theta$ . These parameters were numerically swept with increments  $\Delta\lambda = \Delta\theta = 0.025$ . The grayscale color represents the accuracy score (see Appendix A); the red contours represent regions of high accuracy (above 0.9). The first five columns correspond to different values of the pattern activity  $a$ , whereas the last column shows the overlay of the high-accuracy regions for these different activity levels. The green dots in the  $a = 0.3$  column correspond to the time series shown in Fig. 4.

This suggests that MSI is able to retrieve sequences among patterns with varying activities, which we explore below.

**D. Variability in pattern activity**

So far we have focused on sequential retrieval of patterns with the same activity. To study how well the models can retrieve patterns with different activities, we consider patterns  $\xi^\mu$  which each have a particular activity level  $a_\mu$  (in which case the formulas involving  $a$  are modified to have  $a_\mu$  instead). We choose five patterns with  $a_\mu$  equally spaced within the range  $0.3 \pm 0.2r$ , where the unevenness parameter  $r$  is varied between 0 and 1. Because the patterns have different activities, the order of these patterns in the sequence can affect retrieval. Therefore, we compute the mean accuracy of retrieval over all possible permutations of a given set of patterns (the scores are first binarized according to a cutoff and then averaged).

Figure 6(a) shows the average accuracy as we vary the unevenness. The ratio of the gray area to the retrieval region for uniform patterns (red contour) represents the ability of each model to retrieve uneven patterns. It can be seen that the MSI model is robust to unevenness in pattern activity, as expected from our observation of Fig. 5, as well as to the ordering of the patterns. We quantify this robustness in Fig. 6(b), where the

area of the retrieval region is plotted against the unevenness. While this measurement of robustness decays rapidly for other models, it is much more stable for MSI. Our results are not qualitatively affected by altering the accuracy cutoff, as shown in Fig. 6(c).

**E. Dynamic storage capacity**

So far we have studied sequential retrieval of a small number of patterns. We now study how these models differ in their dynamic capacity, i.e., the ability to retrieve increasingly long sequences of patterns. We quantify the dynamic capacity by the longest sequence of patterns which may be stored by a network of size  $N$ . To this end, we define  $p_c$  as the critical number of patterns beyond which the dynamic accuracy drops below a threshold value, taken to be 0.7. The patterns are randomly generated with the same activity level ( $a = 0.3$ ), and we average the accuracy over 100 sequence realizations.

Figure 7(a) shows the accuracy as a function of the number of patterns for the four models in Table I. As the length of the sequence increases, the retrieval accuracy decreases. However, substantial differences exist in the behavior of these models. For instance, the HU model shows no apparent improvement in its capacity to store longer sequences as the

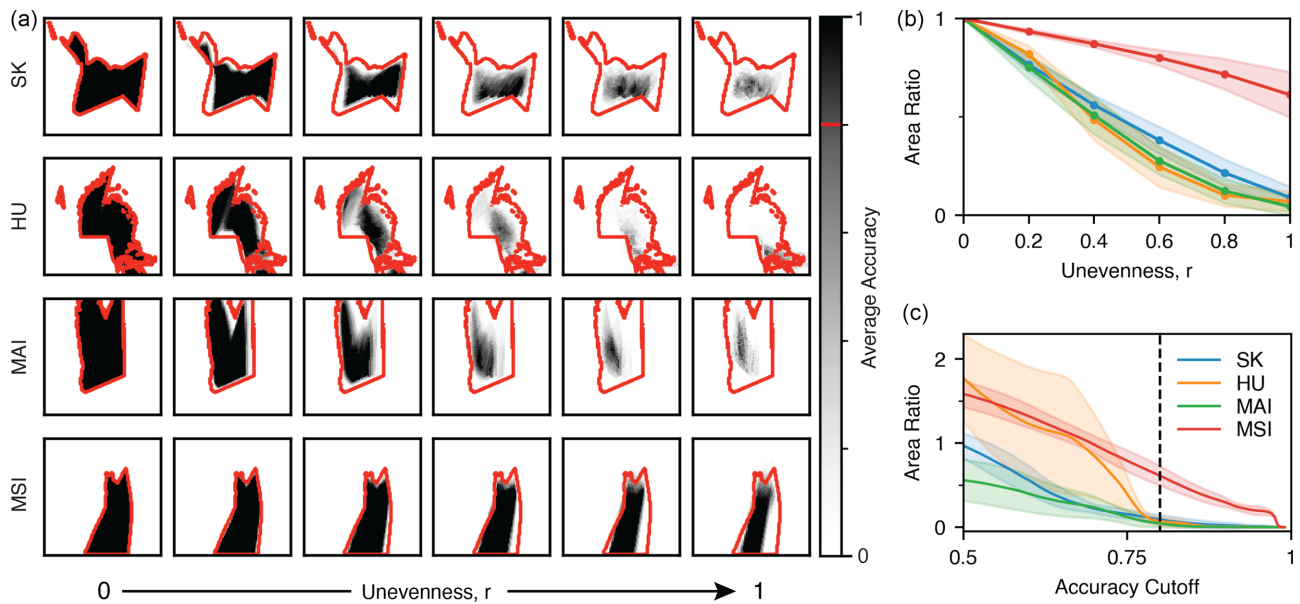


FIG. 6. Retrieval for variable activities and sequence compositions. (a) Phase diagrams are computed for each model at different unevenness of activity levels [ $r$  values as marked in (b)]. The parameter ranges are the same as for Fig. 5. The retrieval accuracy at each point  $(\theta, \lambda)$  is first binarized according to a cutoff of 0.8 and then averaged over all permutations. This average accuracy is colored using a grayscale and the red contours represent the shaded area for  $r = 0$ . (b) The ratio of the gray area to the red contoured region is calculated for each unevenness value  $r$ . The curves show the mean of the area ratios over sequence permutations (for an accuracy cutoff of 0.8) and the color shades show the standard deviations. (c) The area ratio for unevenness  $r = 1$  is calculated as the accuracy cutoff is varied. The dashed line corresponds to a cutoff of 0.8 used in (a) and (b), above which all models fail except MSI.

network size increases. In contrast, the MSI model remains highly accurate for a large number of patterns. To corroborate this observation, we plot the critical number of patterns  $p_c$  against the network size  $N$ , as shown in Fig. 7(b). While the

range of  $N$  is not sufficient to constitute a comprehensive scaling analysis, this figure shows that the MSI model vastly outperforms the other models in terms of dynamic storage capacity.

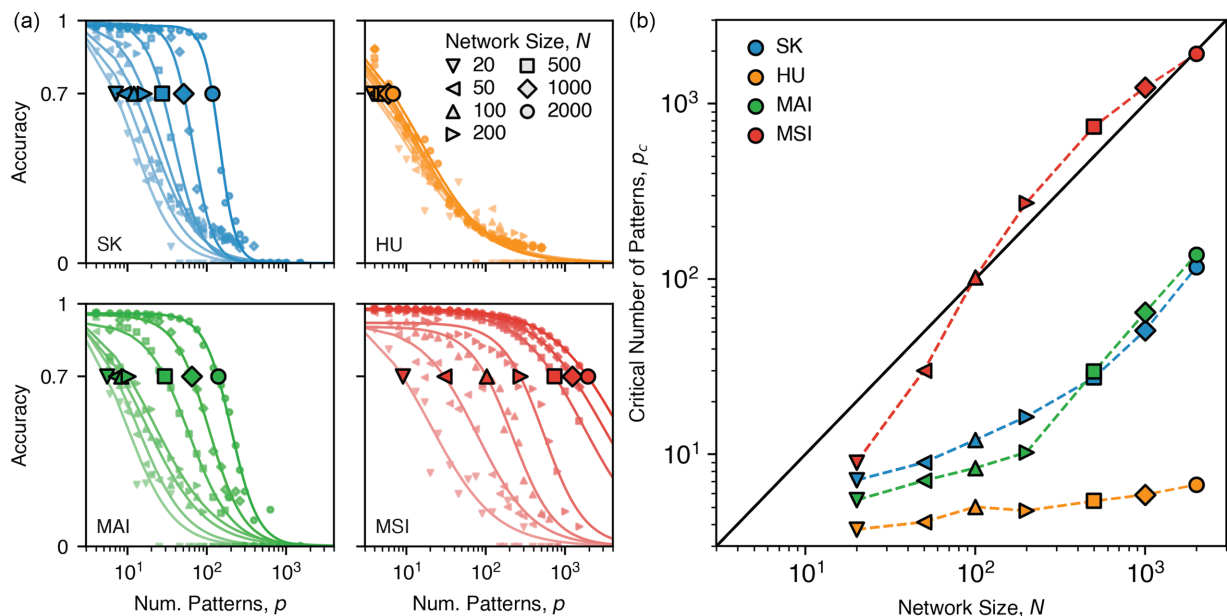


FIG. 7. Dynamic capacity of sequential retrieval. (a) For each network size  $N$ , the average accuracy of retrieval is plotted against the number of patterns  $p$ . The accuracy is calculated for a sequence of  $p$  randomly generated patterns with  $a = 0.3$ , averaged over 100 realizations. A sigmoidal curve is fitted for each  $N$  and the critical number of patterns  $p_c$  is defined as the value of  $p$  where the average accuracy falls below 0.7, indicated by the marker. (b) The estimated values of  $p_c$  are plotted against the size of the network  $N$ , showing different scaling for each model. The parameters used to simulate each model are the same as for Fig. 4 (see caption).

#### IV. DISCUSSION

In this work we have used the Hopfield network as a setup and formulated multiple models capable of sequentially retrieving stored patterns. In our framework, the transition between subsequent patterns is controlled by a set of feedback units, where feedback is coupled either directly to the main units in the case of input modulation or to the interactions between these units in the case of interaction modulation.

Such a structure of a regulatory layer that exerts feedback on a functional layer is common in biology. For example, at the cellular level, self-assembly of protein complexes is controlled by assembly factors [24]; at the neuronal level, motor sequences could be generated from feedback between the thalamus and cortex [25]. In our model we further assumed a separation of timescales between the two layers, which is also motivated by biological examples. In the case of protein complexes, the self-assembly of spliceosome occurs on timescales below a second [26,27], while the processing of pre-mRNA occurs on tens of seconds (BIONID: 108453). For neurons, the thalamic dynamics may happen on much faster timescales than cortical dynamics [25]. Furthermore, feedback in sequential dynamics has also been proposed to occur through processes such as learning of asymmetric interactions [14] or neuronal depression [28,29], both much slower than neuronal firing. Indeed, a separation of timescales is commonly assumed in previous models of sequential dynamics, some of which we discuss below.

##### A. Advantages and drawbacks of interaction modulation

While all models that we studied are capable of sequential retrieval, we showed that an interaction modulation model (MSI) outperforms the others. The MSI model is robust to variations in the activity level of the patterns and the ordering of the sequence and is capable of retrieving much longer sequences than the others. The unique features of the MSI model can be intuitively understood by investigating the local and global stability of the dynamics.

As known from local analysis of the storage capacity of the Hopfield model [30], the retrieval of a pattern can be disrupted by crosstalk between different patterns that are not fully orthogonal to each other. As we show in the Supplemental Material [23], while all models studied here are subject to crosstalk with a similar scaling with network size  $N$  and number of patterns  $p$ , in MSI the crosstalk is relatively suppressed. This is because there is an extra factor of  $c_\mu$  in the crosstalk term, which comes from interaction modulation, and a prefactor  $\lambda$  that is small in MSI. As a result, we expect MSI to have a larger critical number of patterns  $p_c$  before the crosstalk disrupts the retrieval of patterns.

Even for orthogonal patterns, there can be extra local minima in the slowly changing energy landscape that stall the sequential dynamics. To explore such global stability, we added a Gaussian random term to the equation for feedback units, which represents noise in the input or interaction modulation. We simulated the dynamics with  $p = 20$  orthogonal patterns and various levels of noise for the MSI and SK models. Figures S4 and S5 in the Supplemental Material [23] show how the accuracy of sequential retrieval decreases with

the noise level, with MSI being significantly more robust than SK. Such robustness is likely due to the dynamics of the network happening across a less rugged energy landscape than the dynamics of alternative models (Table I). In associative memory networks spurious minima arise as linear combinations of stored patterns. The MSI model, however, stores only a single pattern in  $J_{ij}$  at any moment during sequential retrieval. We therefore expect that dynamics unfold on a smoother landscape, resulting in more accurate retrieval as observed.

Besides these advantages, interaction modulation also exhibits clear drawbacks. The main issue is that each feedback unit has to generate  $O(N^2)$  outputs to modulate all the interactions, as opposed to  $O(N)$  outputs for input modulation. This requirement of large connectivity can be relaxed if we dilute the outputs of the feedback units by suppressing a fraction  $f$  of modulated interactions chosen at random. Figure S6 in the Supplemental Material [23] shows that accurate sequential retrieval can be retained even when up to about half of the feedback outputs are removed in the MSI model. Nonetheless, the number of required connections still scales as  $N^2$ , which poses an undeniable disadvantage in terms of potential implementation of such interaction modulation and complication of learning rules, which we do not explore here.

A general form of interaction modulation by feedback units can be written as  $J_{ij}(c_\mu) = \sum_\mu T_{ij}^\mu c_\mu$ , where  $T_{ij}^\mu$  is some tensor representing how the interaction between two nodes  $(s_i, s_j)$  is modulated by a feedback unit  $c_\mu$ . For example, the MSI model corresponds to  $T_{ij}^\mu \propto (\xi_i^\mu - a)(\xi_j^\mu - a)$ . Such a model generally involves  $O(pN^2)$  parameters, as each feedback unit can modulate the interactions in a different direction. The random dilution of interactions studied above reduces the number of parameters by a factor of  $f$ . Another situation which may be biologically more plausible is when patterns are sparse and localized, which would reduce the number of parameters by a factor of  $a^2$ . We have verified that in this regime MSI still has a clear advantage over SK in terms of dynamic capacity (Supplemental Material [23], Fig. S7).

We may also consider models where individual terms in the interactions are not modulated separately. Two such examples are presented in Appendixes B 2 and B 3, where the feedback units modulate the interactions collectively through a factor  $\phi(\{c_\mu\})$ . In these cases, the number of parameters is reduced to  $O(N^2)$  for determining the overall Hopfield-like connections  $J_{ij}$ . Figure S3 in the Supplemental Material [23] shows that these models are capable of retrieving dynamic sequences. Thus, interaction modulation is a general and versatile paradigm for sequential retrieval, with different implementations that may be suitable for different biological contexts, as we discuss below.

##### B. Relation to previous work

Many models of sequential retrieval, such as those presented in Sec. III A, originate from the study of associative memory and the dynamics of real neurons. For example, in the SK model the role of feedback is played by slow asymmetric interactions [12]. Later models, such as HU, introduced such slow feedback as neural fatigue, modeled as a neuron-specific threshold that increases when the neuron remains active [13].

Another model produces so-called latching dynamics through combining a slow time-dependent threshold with neurons of many internal states [18]. Sequence generation in neural networks has also been modeled using other approaches, such as winnerless competition based on heteroclinic orbits [22,31,32], coherent dynamics from chaotic networks [33], switching-linear dynamical systems [25], and threshold-linear networks based on graph-theoretic methods [34].

Coupling feedback to interactions has been studied in various forms within the context of neural networks. In Ref. [14], the authors are motivated by a type of allosterity among neurons: regulation of the efficacy of a given synapse by the activity of another synapse. Their model allows pairwise interactions to be modified by other neurons in the network and bears resemblance to our MAI model. This phenomenon, by which a synapse that is not currently active can be strengthened or weakened by the firing of a third modulatory neuron, is referred to as heterosynaptic plasticity [7,35–37]. It has inspired network models that can learn sequences through synaptic competition [38]. Other biological phenomena, such as neural fatigue [29], have also inspired models that modulate neural interactions rather than individual thresholds. For example, in Ref. [28] a slow feedback is introduced to depress the synapses between neurons. This model can be reformulated in our framework of interaction modulation similarly to the MSI model, as presented in Appendix B 1. In Ref. [39], synaptic depression is used to control transitions between patterns by externally modulating a global inhibition of all interactions among neurons, which allows for transitions between correlated patterns. Instead of controlling such inhibition externally, we can modify their model to couple the inhibition to a slow feedback and reformulate it within our framework, as presented in Appendix B 2. Besides heterosynaptic plasticity, there is also extensive literature on synaptic modulation through various neurological mechanisms [40], such as tripartite synapses where a synapse between two neurons is dynamically modulated by one or more astrocytes [41,42]. In line with our results, such systems have been shown to exhibit enhanced computational capabilities [43].

Separate from a biological setting, the mechanism that we introduce as feedback appears widely within control theory, where it is typically studied in the context of control through linear input modulation [5,44]. However, interaction modulation is a less studied form of controlling network dynamics [45], especially when the interactions are structured like in the Hopfield network. Our results suggest that interaction modulation may be a new paradigm for controlling nonlinear dynamics.

### C. Potential applications

In this paper we have used the Hopfield network as a modeling framework to describe high-dimensional dynamics that follows a low-dimensional trajectory. The choice of this framework is largely driven by its mathematical simplicity and conceptual clarity. Due to such simplicity, this framework has been instrumental not only in the understanding of associative memory in neuroscience, but also in other biological problems, such as metabolic networks [9] and protein assem-

blies [10]. Furthermore, Hopfield networks have recently been shown to be of practical use in the context of machine learning [46]. Similarly, we expect that our paradigm of interaction modulation can be applied to different fields of biology, with specific implementations suited for given problems. We have described several variants of interaction modulation models, which may pave the way for such applications.

While in the preceding section we discussed the relationship of our work to neuronal systems, an alternative application is the basis for modeling dynamics of heterogeneous protein mixtures. Recent work on protein self-assembly and liquid mixtures [10,47] has shown a direct mapping between multicomponent protein mixtures and neural networks. In this analogy, the role of a neuron is played by a protein species, the interaction matrix  $J_{ij}$  maps to the binding affinity between proteins, the input field  $V_i$  translates to the chemical potential, and the activation state of the neuron  $s_i$  represents either the location of the protein in an assembly or the concentration of the protein in a mixture. In this way, input modulation corresponds to controlling protein assembly dynamics by changes in their chemical potential. This type of regulation is seen, for example, in the sequential assembly of different cell-cycle complexes that contain cyclin and cyclin-dependent kinases, during which the concentrations of these key proteins and their chemical potentials oscillate along the cell cycle [48]. Similarly, interaction modulation is seen in protein assemblies, such as through allosteric interactions common to many regulatory proteins, which allows the affinity between two proteins to depend on the ligand bound to the allosteric site. In this case, the affinity is best described by a tensor  $T_{ij}^\mu$  similar to the MSI model of interaction modulation. Such a model would be complementary to, and in fact more biologically plausible than, other interaction modulation models recently studied in the self-assembly literature [20].

### D. Perspective

In biology, interactions among the components of a system are often effective coarse-grained descriptions of complicated microscopic mechanisms. The strength of such effective interactions can be tuned by modifying the underlying mechanisms. Modification of interaction strengths is quite common among biological systems, such as allosteric regulation of protein interactions [49] and trait-mediated modification of species interactions [50,51], yet the benefits of being able to modify interactions is underexplored theoretically. Here we have demonstrated that interaction modulation can be an effective way of controlling the stability of system configurations and the direction of its dynamics, which may be important for biological functions and evolution.

In complex systems, the interactions among many constituent units give rise to various collective behaviors, such as coherent motion [52–54] or collaborative functions [55]. The sequential transition of the system between multiple metastable configurations that we modeled here is one type of collective behavior, and we have shown that interaction modulation is a robust way of controlling such behavior. Our study may inspire future work on exploring the role of interaction modulation in other situations.

### ACKNOWLEDGMENTS

We thank Tiberiu Tesileanu for valuable feedback on this work and Stanislas Leibler for helpful discussions at the early stages of this work. We also thank anonymous referees for comments that motivated further analyses of the results. P.S. was partly supported by la Caixa under Grant No. LCF/BQ/PI21/11830032.

### APPENDIX A: COMPUTING RETRIEVAL ACCURACY

To evaluate the performance of sequential retrieval over an extended period of time, we introduce a scoring scheme that first calculates instantaneous scores and then averages them over time to produce an overall accuracy. The instantaneous score function is defined for each pattern as

$$S^\mu(\{m^v\}) = \frac{G(m^\mu)}{\sum_v G(m^v) + \epsilon}, \quad (\text{A1})$$

where

$$G(m^\mu) = \frac{\text{expit}(m^\mu; \kappa, \rho) - \text{expit}(-1; \kappa, \rho)}{\text{expit}(1; \kappa, \rho) - \text{expit}(-1; \kappa, \rho)}, \quad (\text{A2})$$

with  $\text{expit}(x; \kappa, \rho) \equiv 1/(1 + e^{-\kappa(x-\rho)})$ . Our construction of  $G(m^\mu)$  attenuates  $m^\mu$  below some threshold  $\rho$  towards 0 and amplifies  $m^\mu$  above  $\rho$  towards 1, so instances of retrieval correspond to a single high  $S^\mu$  when the patterns are orthogonal. The parameters were chosen as  $\kappa = 10$  and  $\rho = 1 - a$  for all analyses, and  $\epsilon = 10^{-5}$  to make the instantaneous score well defined even when  $m^\mu = 0$  for all  $\mu$ .

Each pattern is retrieved and remains stable for a continuous interval of time, which we call an instance of retrieval. We identify such intervals as blocks of time when  $G(m^\mu) \approx 1$ , which corresponds to  $m^\mu > \theta$ . The score of an instance of retrieval amounts to the time average of the instantaneous scores over the interval

$$\bar{S}^\mu = \frac{1}{t_2 - t_1} \int_{t_1}^{t_2} S^\mu(\{m^v\}) dt, \quad (\text{A3})$$

where  $t_1$  and  $t_2$  are the bounds of the interval. The time series of network dynamics is typically composed of many retrieval instances, so we define the overall accuracy of sequential retrieval as the average score over many retrieval instances in the time series. In all cases, the network is simulated with  $\tau = 10$  and  $\Delta t = 0.1$  for 6000 time steps. We compute the accuracy only for the latter half of each time series to avoid the transient dynamics in the beginning.

In the phase-space analysis of Sec. III C we chose a cutoff between high-accuracy and low-accuracy regions of retrieval, indicated by the red contours in Fig. 5. To determine an appropriate accuracy cutoff, we examined the distribution of scores over parameter space  $(\lambda, \theta, a)$  for each model, as shown in Fig. 8. The rightmost peak (corresponding to high-accuracy retrieval) is separated from the remaining peaks by a cutoff accuracy of 0.9.

### APPENDIX B: OTHER MODELS OF INTERACTION MODULATION

Sequential dynamics through interaction modulation can be implemented in models other than those presented in the

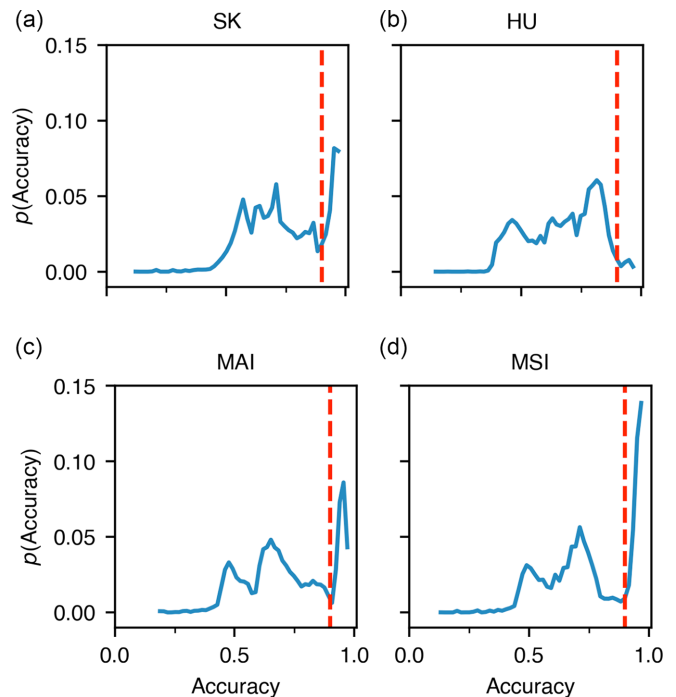


FIG. 8. Accuracy distributions. The distributions of accuracies over the parameter phase space in Fig. 5 are calculated and marginalized over  $a$  for (a) and (b) input modulation and (c) and (d) interaction modulation models. The rightmost peak, corresponding to accurate retrieval, is separated by an accuracy cutoff of 0.9 (only a small peak is present in HU). For clarity, scores of zero are omitted.

main text. Here we provide two more examples in which the symmetric interactions are modulated through mechanisms different from that in MSI, with the rest of the model remaining the same.

#### 1. Complement of the MSI model

In the presented MSI model the symmetric interactions  $J_{ij}$  have dynamics such that at any time only one pattern is accessible, as only one  $c_\mu$  is active. The network retrieves the pattern and, after some time, this pattern is purged from  $J_{ij}$  and a new pattern is stabilized and retrieved. Here we present a complementary model where at any given time all patterns are present in  $J_{ij}$  except one. When the network retrieves one pattern, the corresponding  $c_\mu$  will slowly suppress it in  $J_{ij}$  while all other patterns remain. This model can be described similarly to MSI in Table I except that

$$J_{ij}(c_\mu) = \frac{1}{Na(1-a)} \sum_\mu (\xi_i^\mu - a)(\xi_j^\mu - a)(1 - c_\mu). \quad (\text{B1})$$

When  $c_\mu$  increases and  $\xi^\mu$  is no longer stable, the network will be pushed towards the next pattern  $\xi^{\mu+1}$  by the asymmetric interactions  $\tilde{J}_{ij}$  as in MSI. This model is similar in spirit to that studied in Ref. [28], where part of the symmetric interactions is depressed after a pattern is retrieved for some time. Example dynamics for the complement of MSI are shown in the Supplemental Material [23], Fig. S3A.

## 2. Global inhibition

Another form of interaction modulation has been considered in Ref. [39], where the symmetric interactions take the form

$$J_{ij} = \frac{1}{Na(1-a)} \left( \sum_{\mu} (\xi_i^{\mu} - a)(\xi_j^{\mu} - a) - \phi \right). \quad (\text{B2})$$

In this equation, the parameter  $\phi$  represents a global inhibition of all symmetric interactions. This parameter is externally controlled to oscillate between a minimum value at which patterns can be retrieved and a maximum value at which only part of the previously retrieved pattern can remain active. When  $\phi$  is reduced again, the next pattern retrieved will be the one that has the largest intersection with the active part [39].

In order to adapt this model to exhibit sequential dynamics, we modify it so that the global inhibition  $\phi$  is modulated through feedback, rather than externally. In particular, we consider

$$\phi = \theta \sum_{\mu} f(c_{\mu}), \quad (\text{B3})$$

where the parameter  $\theta$  controls the maximum inhibition strength. Together with the asymmetric interactions as described in Table I for MSI, this model is capable of sequential

retrieval. Example dynamics for the modified global inhibition model are shown in the Supplemental Material [23], Fig. S3B.

## 3. Global interaction suppression

Another model similar to Eq. (B2) can be formulated as

$$J_{ij} = \frac{\phi}{Na(1-a)} \sum_{\mu} (\xi_i^{\mu} - a)(\xi_j^{\mu} - a), \quad (\text{B4})$$

where

$$\phi = 1 - \theta \sum_{\mu} f(c_{\mu}). \quad (\text{B5})$$

In this model, the symmetric interactions are modulated by an overall factor  $\phi$ , which is controlled by the feedback units. Here  $f(\cdot)$  is a nonlinear activation function with a threshold at  $1 - a$ , and  $\theta$  is a parameter controlling the global suppression of symmetric interactions. When a pattern has been retrieved for some time, the factor  $\phi$  is reduced to suppress the stabilizing effect of the symmetric interactions. In the presence of small asymmetric interactions, the system will be destabilized and pushed towards the next pattern. Example dynamics for this model are shown in the Supplemental Material [23], Fig. S3C.

- 
- [1] G. V. Wallenstein, M. E. Hasselmo, and H. Eichenbaum, The hippocampus as an associator of discontinuous events, *Trends Neurosci.* **21**, 317 (1998).
  - [2] H. Eichenbaum, Memory on time, *Trends Cognit. Sci.* **17**, 81 (2013).
  - [3] M. C. Wahl, C. L. Will, and R. Lührmann, The spliceosome: Design principles of a dynamic RNP machine, *Cell* **136**, 701 (2009).
  - [4] M. S. Datta, E. Sliwerska, J. Gore, M. F. Polz, and O. X. Cordero, Microbial interactions lead to rapid micro-scale successions on model marine particles, *Nat. Commun.* **7**, 11965 (2016).
  - [5] Y.-Y. Liu and A.-L. Barabási, Control principles of complex systems, *Rev. Mod. Phys.* **88**, 035006 (2016).
  - [6] S. J. Wodak *et al.*, Allosteric in its many disguises: From theory to applications, *Structure* **27**, 566 (2019).
  - [7] C. H. Bailey, M. Giustetto, Y.-Y. Huang, R. D. Hawkins, and E. R. Kandel, Is heterosynaptic modulation essential for stabilizing hebbian plasticity and memory, *Nat. Rev. Neurosci.* **1**, 11 (2000).
  - [8] J. J. Hopfield, Neural networks and physical systems with emergent collective computational abilities, *Proc. Natl. Acad. Sci. USA* **79**, 2554 (1982).
  - [9] A. De Martino, D. De Martino, R. Mulet, and G. Uguzzoni, Reaction networks as systems for resource allocation: A variational principle for their non-equilibrium steady states, *PLoS ONE* **7**, e39849 (2012).
  - [10] P. Sartori and S. Leibler, Lessons from equilibrium statistical physics regarding the assembly of protein complexes, *Proc. Natl. Acad. Sci. USA* **117**, 114 (2020).
  - [11] D. A. Power, R. A. Watson, E. Szathmáry, R. Mills, S. T. Powers, C. P. Doncaster, and B. Czapp, What can ecosystems learn? Expanding evolutionary ecology with learning theory, *Biol. Direct* **10**, 69 (2015).
  - [12] H. Sompolinsky and I. Kanter, Temporal association in asymmetric neural networks, *Phys. Rev. Lett.* **57**, 2861 (1986).
  - [13] D. Horn and M. Usher, Neural networks with dynamical thresholds, *Phys. Rev. A* **40**, 1036 (1989).
  - [14] S. Dehaene, J.-P. Changeux, and J.-P. Nadal, Neural networks that learn temporal sequences by selection, *Proc. Natl. Acad. Sci. USA* **84**, 2727 (1987).
  - [15] J. Buhmann and K. Schulten, Noise-driven temporal association in neural networks, *Europhys. Lett.* **4**, 1205 (1987).
  - [16] D. Kleinfeld and H. Sompolinsky, Associative neural network model for the generation of temporal patterns. Theory and application to central pattern generators, *Biophys. J.* **54**, 1039 (1988).
  - [17] D. J. Amit, Neural networks counting chimes, *Proc. Natl. Acad. Sci. USA* **85**, 2141 (1988).
  - [18] E. Russo and A. Treves, Cortical free-association dynamics: Distinct phases of a latching network, *Phys. Rev. E* **85**, 051920 (2012).
  - [19] M. Naim, M. Katkov, S. Romani, and M. Tsodyks, Fundamental law of memory recall, *Phys. Rev. Lett.* **124**, 018101 (2020).
  - [20] S. Osat and R. Golestanian, Non-reciprocal multifarious self-organization, *Nat. Nanotechnol.* **18**, 79 (2023).
  - [21] H. Sompolinsky, A. Crisanti, and H.-J. Sommers, Chaos in random neural networks, *Phys. Rev. Lett.* **61**, 259 (1988).
  - [22] P. Seliger, L. S. Tsimring, and M. I. Rabinovich, Dynamics-based sequential memory: Winnerless competition of patterns, *Phys. Rev. E* **67**, 011905 (2003).

- [23] See Supplemental Material at <http://link.aps.org/supplemental/10.1103/PRXLife.1.023012> for analytical and numerical arguments for the robustness of interaction-modulation models as compared to input-modulation models and for additional figures illustrating detailed aspects of such robustness.
- [24] D. Kressler, E. Hurt, and J. Baßler, Driving ribosome assembly, *BBA Mol. Cell. Res.* **1803**, 673 (2010).
- [25] L. Logiaco, L. Abbott, and S. Escola, Thalamic control of cortical dynamics in a model of flexible motor sequencing, *Cell Rep.* **35**, 109090 (2021).
- [26] C. L. Will and R. Lührmann, Spliceosome structure and function, *Cold Spring Harbor Perspect. Biol.* **3**, a003707 (2011).
- [27] M. Huranová, I. Ivani, A. Benda, I. Poser, Y. Brody, M. Hof, Y. Shav-Tal, K. M. Neugebauer, and D. Staněk, The differential interaction of snRNPs with pre-mRNA reveals splicing kinetics in living cells, *J. Cell Biol.* **191**, 75 (2010).
- [28] L. Pantic, J. J. Torres, H. J. Kappen, and S. C. Gielen, Associative memory with dynamic synapses, *Neural Comput.* **14**, 2903 (2002).
- [29] H. Markram and M. Tsodyks, Redistribution of synaptic efficacy between neocortical pyramidal neurons, *Nature (London)* **382**, 807 (1996).
- [30] J. A. Hertz, *Introduction to the Theory of Neural Computation* (CRC Press, Boca Raton, 2018).
- [31] M. Rabinovich, A. Volkovskii, P. Lecanda, R. Huerta, H. D. I. Abarbanel, and G. Laurent, Dynamical encoding by networks of competing neuron groups: Winnerless competition, *Phys. Rev. Lett.* **87**, 068102 (2001).
- [32] V. S. Afraimovich, M. I. Rabinovich, and P. Varona, Heteroclinic contours in neural ensembles and the winnerless competition principle, *Int. J. Bifurcat. Chaos* **14**, 1195 (2004).
- [33] D. Sussillo and L. F. Abbott, Generating coherent patterns of activity from chaotic neural networks, *Neuron* **63**, 544 (2009).
- [34] C. Parmelee, J. L. Alvarez, C. Curto, and K. Morrison, Sequential attractors in combinatorial threshold-linear networks, *SIAM J. Appl. Dyn. Syst.* **21**, 1597 (2022).
- [35] H. Z. Shouval, G. C. Castellani, B. S. Blais, L. C. Yeung, and L. N. Cooper, Converging evidence for a simplified biophysical model of synaptic plasticity, *Biol. Cybern.* **87**, 383 (2002).
- [36] Y. Wang, H. Markram, P. H. Goodman, T. K. Berger, J. Ma, and P. S. Goldman-Rakic, Heterogeneity in the pyramidal network of the medial prefrontal cortex, *Nat. Neurosci.* **9**, 534 (2006).
- [37] T. E. Chater and Y. Goda, My Neighbour Hetero-deconstructing the mechanisms underlying heterosynaptic plasticity, *Curr. Opin. Neurobiol.* **67**, 106 (2021).
- [38] I. R. Fiete, W. Senn, C. Z. Wang, and R. H. Hahnloser, Spike-time-dependent plasticity and heterosynaptic competition organize networks to produce long scale-free sequences of neural activity, *Neuron* **65**, 563 (2010).
- [39] S. Recanatesi, M. Katkov, and M. Tsodyks, Memory states and transitions between them in attractor neural networks, *Neural Comput.* **29**, 2684 (2017).
- [40] T. F. Burns and T. Fukai, Simplicial hopfield networks, in *Proceedings of the 11th International Conference on Learning Representations, Kigali, 2023* (ICLR, La Jolla, 2023), [arXiv:2305.05179](https://arxiv.org/abs/2305.05179).
- [41] G. Perea, M. Navarrete, and A. Araque, Tripartite synapses: Astrocytes process and control synaptic information, *Trends Neurosci.* **32**, 421 (2009).
- [42] R. Min, M. Santello, and T. Nevian, The computational power of astrocyte mediated synaptic plasticity, *Front. Comput. Neurosci.* **6**, 93 (2012).
- [43] L. Kozachkov, K. V. Kastanenko, and D. Krotov, Building transformers from neurons and astrocytes, *Proc. Natl. Acad. Sci. USA* **120**, e2219150120 (2023).
- [44] J. Bechhoefer, *Control Theory for Physicists* (Cambridge University Press, Cambridge, 2021).
- [45] T. Nepusz and T. Vicsek, Controlling edge dynamics in complex networks, *Nat. Phys.* **8**, 568 (2012).
- [46] D. Krotov and J. J. Hopfield, Unsupervised learning by competing hidden units, *Proc. Natl. Acad. Sci. USA* **116**, 7723 (2019).
- [47] W. Zhong, D. J. Schwab, and A. Murugan, Associative pattern recognition through macro-molecular self-assembly, *J. Stat. Phys.* **167**, 806 (2017).
- [48] B. Alberts, *Molecular Biology of the Cell* (Garland Science, New York, 2017).
- [49] R. Phillips, *The Molecular Switch* (Princeton University Press, Princeton, 2020).
- [50] J. T. Wootton, The nature and consequences of indirect effects in ecological communities, *Annu. Rev. Ecol. Syst.* **25**, 443 (1994).
- [51] J. C. D. Terry, R. J. Morris, and M. B. Bonsall, Trophic interaction modifications: An empirical and theoretical framework, *Ecol. Lett.* **20**, 1219 (2017).
- [52] T. Vicsek, A. Czirók, E. Ben-Jacob, I. Cohen, and O. Shochet, Novel type of phase transition in a system of self-driven particles, *Phys. Rev. Lett.* **75**, 1226 (1995).
- [53] J. Toner and Y. Tu, Flocks, herds, and schools: A quantitative theory of flocking, *Phys. Rev. E* **58**, 4828 (1998).
- [54] T. Vicsek and A. Zafeiris, Collective motion, *Phys. Rep.* **517**, 71 (2012).
- [55] H. Hashimura, Y. V. Morimoto, M. Yasui, and M. Ueda, Collective cell migration of dictyostelium without cAMP oscillations at multicellular stages, *Commun. Biol.* **2**, 34 (2019).